

18F-Fluorodeoxyglucose PET/CT and Dynamic Contrast-Enhanced MRI as Imaging

Biomarkers in Malignant Pleural Mesothelioma

David O Hall^{a, b}, Clare E Hooper^{c, d, e}, Julie Searle^{a, f}, Michael Darby^g, Paul White^h, John E Harvey^d,
Jeremy P Braybrookeⁱ, Nick A Maskell^{c, d}, Vidan Masani^j, Iain Douglas Lyburn^{a, f}

Affiliations:

- a. Cobalt Health, Thirlestaine Road, Cheltenham, GL53 7AS, UK.
- b. Department of Medical Physics and Bioengineering, University Hospitals Bristol NHS Foundation Trust, Bristol BS2 8HW, UK.
- c. Academic Respiratory Unit, School of Clinical Sciences, University of Bristol, Bristol BS10 5NB, UK.
- d. Pleural Clinical Trials Unit, North Bristol Lung Centre, Southmead Hospital, Bristol, BS10 5NB, UK
- e. Respiratory Medicine Department, Worcester General Hospital, Worcester WR5 1DD, UK.
- f. Radiology Department, Cheltenham General Hospital, Sandford Road, Cheltenham, Gloucestershire, GL53 7AN, UK.
- g. Imaging Department, Southmead Hospital, North Bristol NHS Trust, Bristol BS10 5NB, UK.
- h. Applied Statistics Group, University of the West of England, Coldharbour Lane, Bristol, BS16 1QY, UK.
- i. Bristol Haematology and Oncology Centre, University Hospitals Bristol NHS Foundation Trust, Bristol BS2 8ED, UK.
- j. Department of Respiratory Medicine, Royal United Hospitals, Bath, BA1 3NG, UK.

**Correspondence:

Dr David Hall

Head of Nuclear Medicine Physics Group,

Department of Medical Physics and Bioengineering,

Bristol Royal Infirmary,

Bristol BS2 8HW,

UK.

d.o.hall@bristol.ac.uk Tel: +441173424756

ABSTRACT

Purpose

To compare the use of ^{18}F -fluorodeoxyglucose positron emission tomography with computed tomography (FDG PET/CT) and Dynamic Contrast-Enhanced Magnetic Resonance Imaging (DCE-MRI) to predict prognosis and monitor treatment in Malignant Pleural Mesothelioma.

Methods

FDG PET/CT and DCE-MRI studies carried out as part of the South West Area Mesothelioma Pemetrexed (SWAMP) trial were used. FDG PET/CT and DCE-MRI studies were carried out before treatment, and after two cycles of chemotherapy, on patients treated with Pemetrexed and Cisplatin. 73 patients were recruited, of whom 65 had PET/CT and DCE-MRI scans. Baseline measurements from FDG PET/CT (SUVmax, Metabolic Tumour Volume (MTV) and Total Lesion Glycolysis (TLG)) and DCE-MRI (Integrated Area Under the first 90s of the curve (IAUC90) and washout slope) were compared with overall survival (OS) using Kaplan Meier and Cox regression analysis, and change in imaging measurements were compared with disease progression.

Results

PET/CT and DCE-MRI measurements were not correlated with each other. SUVmax, MTV and TLG were significantly related to OS with Cox Regression and analysis and Kaplan-Meier analysis, and DCE-MRI washout curve shape was significantly related to overall survival. DCE-MRI curve shape can be combined with FDG PET/CT to give additional prognostic information. Changes in measurements were not related to progression free survival.

Conclusions

FDG-PET/CT and DCE-MRI give prognostic information in Malignant Pleural Mesothelioma. Neither PET/CT nor DCE-MRI are useful for monitoring disease progression.

Introduction

Malignant Pleural Mesothelioma (MPM) is caused by exposure to asbestos dust. There is a long latency period, typically 30 to 40 years, between exposure and development of the disease, so incidence continues to rise long after asbestos use has finished. Death rates in Great Britain have continued to increase [1], from 24.6 per million for men and 3.3 per million for women in 1984-1986, to 68.2 and 12.7 deaths per million in 2011-2013; death rates are expected to level off over the next decade. Patients with MPM have a life expectancy of only 9-14 months following diagnosis [2]. Chemotherapy with Pemetrexed and Cisplatin [3] has been shown to have a significant survival benefit.

The South West Area Mesothelioma and Pemetrexed Trial (SWAMP) [4] was designed to examine the use of imaging with ¹⁸F-Fluorodeoxyglucose PET/CT to predict overall survival from baseline imaging, and to correlate changes in PET/CT with progression free-survival. Dynamic Contrast-Enhanced MRI (DCE-MRI) was carried out on patients on the same day as PET/CT, but not used as a primary or secondary outcome measure due to the lack of established evidence to define responders and non-responders. The aim of this sub-study is to compare FDG-PET/CT and DCE-MRI parameters at baseline, in comparison with overall survival, and compare change with radiological progression.

Materials and Methods

Patients

73 patients with biopsy proven MPM were recruited over three years from 2008 to 2011 at seven centres under the South West Area Mesothelioma and Pemetrexed (SWAMP) trial [4]. Ethical and regulatory approval for the study was obtained before recruitment commenced (UK REC Reference: 08/H0102/46), and all subjects signed a written informed consent form. The trial was registered in the UK national portfolio (UKCRN ID:8450). Inclusion criteria were a life expectancy exceeding three months, and no previous debulking surgery or other radical therapy.

All patients were offered chemotherapy with Pemetrexed and Cisplatin or Carboplatin by the oncologist responsible for their clinical care. 58 patients had chemotherapy, while 15 patients who declined chemotherapy received best supportive care. Overall Survival (OS) was measured from recruitment until death or the study closed, 12 months after the last patients were recruited. All patients were offered imaging at study entry and after 6 weeks, following two cycles of chemotherapy.

Imaging

FDG PET/CT scans and DCE-MRI scans were conducted in the same half-day appointment at a single imaging centre; all patients were offered both. The DCE-MRI scan was undertaken before the FDG PET/CT to minimise radiation exposure of clinical staff. Trial scans were stored without direct

identification to the patient and results were not accessible to oncologists responsible for their care.

Progression was determined from CT scans carried out separately, but scored centrally, using the modified RECIST criteria [5].

DCE-MRI

Patients were screened for contraindications to MRI scanning by both the clinical trials team and experienced radiographers, and imaged on a 1 Tesla High Field Open System (Philips Medical Systems, Best, The Netherlands).

Patients were scanned using a fat-saturated T1W axial sequence covering the entire lungs from just above the apices to just below the bases – usually achieved with around 70 contiguous slices of 4mm thickness. There were 20 phases – 1 pre-contrast and 19 post-contrast. The frame time was 45-55s, depending on the imaging field of view. 15ml Gadolinium-based contrast (gadoteric acid) was injected at a rate of 1ml per sec.

PET/CT acquisition

PET/CT scans were performed using a Gemini – GXL scanner (Philips Medical Systems, Best, The Netherlands) with Brilliance 16 slice CT. Patients were nil by mouth for 6 hours prior to the injection of 400 MBq FDG. Blood sugar was checked to be within normal range prior to injection. A 90-minute uptake period was allowed. PET images were corrected for photon attenuation using the CT scan and normalized by body weight. The QA of the PET/CT scanner was carried out according to best accepted practice in the UK.

DCE-MRI image and curve analysis

A method for Region of Interest (ROI) definition was developed, based on Giesel et al [6, 7]. A similar method has been described for a study of Zoledronic acid in pleural disease [8]. The tumor was identified on the T1 image (figure 1A), taking account of the enhancement image by a consensus of two radiologists experienced in DCE-MRI analysis. A freehand ROI was defined on a single slice around the pleural tumor at the level with the largest clearly definable area of tumor on the Philips workstation, taking care to exclude normal lung. A graph of image intensity against frame was generated for each ROI and image sequence (figure 1B).

The curve data was transferred as a text file from the Philips workstation to a spreadsheet programme (Microsoft Excel). The time from baseline image to the first enhanced image varied, so $t=0$ was taken to be one frame length before the first enhancement point.

From the percentage enhancement-time curve the Integrated Area Under Curve in the first 90s (IAUC90) and the washout slope (change in percent enhancement/minute) from 4-8 minutes were calculated. The area under the curve was calculated using the trapezium rule, and the change between data points was assumed to be linear for calculations of area under curve. The washout slope was further defined as being type 1 if the enhancement increased by $\geq 1\%$ from 4-8 minutes (slope $> 0.25\%/minute$), type 3 if the enhancement decreased by $\geq 1\%$ from 4-8 minutes (slope $< -0.25\%/minute$), and type 2 if the enhancement neither increased nor decreased (slope between -0.25% and $+0.25\%/minute$).

FDG PET/CT Image Analysis

The tumour VOI was defined as all voxels with a Standardised Uptake Value (SUV) greater than 2.5 [9] within both lungs; this could include discontinuous volumes in diffuse disease. This was edited using tools within MIM software version 5 (MIMvista Corp., Cleveland, Ohio, USA), to remove physiological areas of uptake such as myocardium (figure 2). The following parameters were derived from the images: maximum SUV (SUVmax), Metabolic Tumour Volume (MTV) and Total Lesion Glycolysis (TLG = MTV x mean SUV).

Statistical analysis

Statistics were calculated using the statistical package R [10]. Baseline comparisons between DCE-MRI and PET/CT measurements were carried out on all patients, while survival analysis and comparison with progression-free survival were carried out on chemotherapy patients. Kaplan-Meier estimates for OS were generated using the survival package of R [11]. Significance of differences in Kaplan-Meier analysis was tested using the log-rank test. Kaplan-Meier statistics were calculated comparing values above and below group median for TLG, SUVmax, MTV and IAUC90, and comparing slope types for DCE-MRI washout curves. A p value of 0.05 was taken to be significant, and multiple comparisons were corrected for using the Holm-Bonferroni correction.

Results

Patients

73 patients were recruited between September 2008 and December 2011; 58 were recruited to the chemotherapy arm and 15 to the comparator arm. Of these, 65 had baseline PET/CT (51 chemotherapy arm; 4 withdrew from the trial, 3 were unable to tolerate scans, and 1 was too unwell) and 61 had baseline DCE-MRI scans available (50 chemotherapy arm; 4 sets of data were unable to be analysed for technical reasons). 54 patients had follow-up PET/CT (41 chemotherapy arm; 4 had problems with chemotherapy, 1 was unable to tolerate scans, 3 were too unwell, 1 died, 2 corrupted scans) and 47 had follow-up DCE-MRI available for analysis (37 chemotherapy arm; 7 studies were unable to be analysed). Median follow-up time was 892 days (IQR 605-1144 days); 12 patients were alive at the time of analysis. Patient characteristics are shown in table 1.

Clinical Outcomes

Median survival from consent to death in the chemotherapy group was 368 days (IQR 195–526) and in the comparator group 325 days (IQR 176–458) equating to 12.3 and 10.8 months, respectively ($p=.40$). The number of chemotherapy cycles delivered was determined by oncologists using standard clinical assessment without access to serum biomarkers or PET/CT results. 87% of patients in the chemotherapy group received two or more cycles, 64% received four or more cycles and 36% received six cycles. Histological subtype was a strong independent predictor of survival, with epithelioid histology associated with a median survival of 456 (IQR

303–609) days compared with 197 (IQR 155–239) days ($p < 0.001$) in patients with non-epithelioid histology.

Comparison between PET/CT and DCE-MRI

Baseline measurements from PET/CT and DCE-MRI were compared with each other for all patients, treated and control group. From PET/CT, SUVmax, TLG and MTV were correlated ($p < .0001$) and from DCE-MRI IAUC90 and Washout slope were correlated ($p = .003$). There were no significant correlations of SUVmax with IAUC90 (figure 3, $r = .25$, $p = .055$) or Washout Slope (figure 4, $r = -.17$, $p = .19$), MTV with IAUC90 ($r = .12$, $p = .36$) or Washout slope ($r = -.14$, $p = .30$), or TLG with IAUC90 ($r = .15$, $p = .27$) or washout slope ($r = -.16$, $p = .22$). There were no significant correlations when subgroups were tested with or without pleurodesis, or with epithelioid or non-epithelioid histology.

Comparison with overall survival

Baseline measurements from PET/CT and DCE-MRI were compared with overall survival for treated patients.

From Univariate Cox Regression analysis, the only significant factors were histology and SUVmax, MTV and TLG from PET/CT (table 2). In multivariate analysis, if histology was included no other factors were significant; if histology was excluded then SUVmax was most significant.

All PET/CT measurements showed a significant relationship with overall survival by Kaplan-Meier analysis, comparing values above and below median. SUVmax above median (10.6) had OS 268 (177-481) days, below

median 525 (270-735) days ($p=0.001$) (figure 5); MTV above median (460 mm^3) had median OS 264 (IQR 177-439) days, below median MTV had median OS 562 (274-735) days ($p=0.0001$); and TLG above median (1806 SUV-mm^3) had OS 264 (177-439) days, below median 562 (274-735) days ($p=0.0001$).

For DCE-MRI, baseline IAUC90 was not significantly related to OS (figure 6); iAUC90 above median (88 %-min) gave median OS 270 (IQR 232-507) days, below median 506 (250-735) days ($p=0.07$). Washout slope was significantly related to OS (figure 7): type 1 ($n=13$) median OS 562 days (IQR 481-872) days, type 2 ($n=6$) median OS 256 days (IQR 104-498) days, type 3 ($n=31$) median OS 274 (204-525) days; $p=0.023$.

Combining PET/CT SUVmax and DCE-MRI Washout slope gave additional information (table 3). Those with SUVmax <10.6 and type 1 curves had the longest survival, median OS 735 days, SUVmax <10.6 and type 2 or 3 curves had median OS 426 and 401 days, while patients with SUVmax >10.6 had median OS 312, 130 and 268 days for type 1, 2 and 3 curves respectively ($p=.009$). Numbers in each group were too small to calculate confidence intervals for OS.

There was no significant difference in OS between those who had and had not had pleurodesis.

Comparison with Progression from CT

Change in PET/CT (SUVmax, MTV and TLG) and DCE-MRI (IAUC90, Washout slope) were compared with progression-free survival at 8 weeks (table 4), 15 weeks (table 5), and 12 months (table 6). Change in washout

slope at 7-9 weeks and MTV and TLG at 9 months were significant at the $p < .05$ level, though correcting for multiple comparisons these were not significant ($p < .003$ required for 15 comparisons).

Discussion

MRI of the lungs is difficult due to breathing-related motion artefact. As a consequence of this, the slice on which the analysis is carried out moves relative to the tumour between time-points, and so the enhancement-time curves were somewhat noisy. However, the advantage of using the area under the curve and the washout slope is that the effect of movement on these measurements should be limited, as movement will effectively be smoothed out. PET/CT is also subject to movement, which can be seen from the mismatch between the PET and the CT particularly at the lung bases. This will cause the uptake to be somewhat smoothed, with a potential reduction in SUVmax. This should have limited effect on the volumetric measures in most cases, unless the uptake is close to the threshold. A fixed SUV threshold was used to analyse PET images as this is a method which is widely available, and does not require specialised software. The other method most widely used, a threshold at around 40% of maximum, would not be appropriate for diffuse tumour, as this is a method which has been validated for discrete solid tumours. In some cases there was visible tumour on PET/CT which was below the threshold of $SUV=2.5$ and so was not included in the MTV. However, these cases would have low FDG uptake however measured, which would be correlated with relatively long survival times.

The analysis used for PET was fully 3D and took account of all active tumour throughout both lungs. On the other hand, the method for MRI was based on analysis of data from a single slice through the largest volume of

tumour. The largest tumour volumes corresponded for MRI and PET, however the SUVmax did not necessarily lie at the same point as the centre of the MRI ROI, although it often would have done. It would clearly be preferable to have used more comparable 3D analysis methods in both cases. However, the different measurements from PET/CT, SUVmax, MTV and TLG, were strongly correlated, suggesting that the overall tumour function can be measured using a measurement of uptake at a single voxel. This suggests that the difference between 2D and 3D analysis may not be too significant in this case. There was also no attempt to register studies before and after treatment, and image analysis was performed separately for pre and post-treatment studies.

Probably of most importance is the different physiological and pathological meaning of the results. DCE-MRI is a measure of perfusion, while FDG-PET/CT is a measure of metabolism. The results indicate that more active tumour tends to have higher perfusion, but that the metabolism from SUVmax or TLG is more significantly related to overall survival. SUVmax from PET/CT and curve-shape from DCE-MRI were combined (table 3); in this case, SUVmax was the most significant factor, as patients with SUVmax < median (10.6) had longer survival than those with SUVmax > median for all DCE-MRI curve shapes, but within this curve shape 1 generally gave longer survival than curve shapes 2 or 3.

A number of previous studies [9, 13-20], mostly retrospective and observational, have considered the relationship between survival and PET measurements at baseline. Of these, 8 studies [13-20] with a total of 594 patients found that high SUVmax or TLG at baseline indicated worse

survival, and one with 41 patients [9] found no relationship. Three studies have considered percentage change in SUVmax, TLG and MTV after chemotherapy; two [9,12] with a total of 64 patients found that a percentage reduction in TLG was indicative of better OS, while one [20] with 131 patients found a percentage reduction in SUVmax was related to longer OS. Prior pleurodesis has also been indicated as an issue, causing raised SUVmax in some studies [21, 22], but this was not found in our study.

Previous work on the use of DCE-MRI in MPM used a pharmacokinetic modelling method to analyse studies on 19 patients with epithelioid histology, and showed longer OS for patients with a lower redistribution rate constant [6,7] though this was not significant.

The utility of DCE-MRI in MPM with enhancement-time curves and curve-based analysis is well established in breast cancer trials [23], while the curve shape and particularly the washout slope are used in clinical assessment of DCE-MRI studies in breast cancer [24]. Currently DCE-MRI is not used in routine clinical practice in evaluating lung or pleural malignancy. It has not been extended into clinical practice partly due to technical difficulties of respiration and the complex morphological characteristics of the lesions. In this study there was a trade-off between anatomical coverage and temporal resolution. Dynamic sequences were acquired for up to 12 minutes in order to assess washout, but shorter frame times would be better for analysis of initial enhancement.

Quantification of DCE-MRI has only occasionally been carried out in MPM. One reason may be the complexity of the pharmacokinetic approach. We

have shown that it is possible to derive measurements from DCE-MRI without specialised software or acquisition parameters. Simple curve-based measurements from DCE-MRI have been shown to be related to pharmacokinetic measurements which can be generated from model-based analysis [25], while pharmacokinetic measurements have been shown to be correlated with microvascular density in MPM [7].

The SWAMP study recruited patients from 7 centres. However, PET/CT imaging was only available at one centre, so all PET and MRI imaging was carried out there. This created issues for recruitment and follow-up imaging, due to the poor health of the participants and the distance from some recruiting centres. There were also some issues with archiving of image data, particularly for DCE-MRI. There were still sufficient numbers for analysis, but subgroup analysis, for example by histology, was more difficult. In the MRI studies due to the fairly long frame length used (45-55s), information may have been lost about initial enhancement, although this should not have affected the analysis used of initial area under curve and washout slope significantly. The MRI studies were carried out on a 1T scanner, and a more modern 3T scanner would be able to image the lungs with a shorter frame time. Due to underlying disease, breath holding was difficult, so the bases of the lungs particularly were affected by movement. Other semi-quantitative measures for DCE-MRI have been proposed, including pharmacokinetic analysis, and it is possible that different methodology might make a difference. Alternatively, perfusion could be assessed by using contrast enhanced CT, which could be carried out as part of the PET/CT study. It would be of interest to compare the results of

perfusion assessment from CT and DCE-MRI in these patients. MRI will often be used as part of the diagnostic or patient management pathway, and in this case it might be appropriate to include assessment of DCE-MRI.

Conclusion

We have demonstrated that FDG-PET/CT and DCE-MRI can be quantified using relatively simple methods in a clinical setting, and that DCE-MRI carried out before treatment may offer prognostic information additional to that from FDG PET/CT. Baseline measurements of SUVmax, MTV and TLG from FDG PET/CT were significantly related to overall survival. Baseline washout curve shape from DCE-MRI was significantly related to overall survival, and offered additional prognostic information when combined with PET/CT, although the PET/CT result was more clinically significant. No measurements of change after treatment from FDG PET/CT or DCE-MRI were related to progression-free survival, so PET/CT and DCE-MRI are not recommended for follow-up in MPM.

PET/CT gives prognostic information in Malignant Pleural Mesothelioma. DCE-MRI gives some prognostic information, but PET/CT should be used instead of DCE-MRI where available.

References:

1. HSE – UK Health and Safety Executive (2016). Mesothelioma.
Available at:
www.hse.gov.uk/Statistics/causdis/mesothelioma/index.htm accessed
June 2016.
2. Chapman A, Mulrennan S, Ladd B, Muers MF. Population-based
epidemiology and prognosis of mesothelioma in Leeds, UK. *Thorax*
2009; 63:435-439.
3. National Institute for Health and Care Excellence. Pemetrexed for the
treatment of malignant pleural mesothelioma. Technology Appraisal
Guidance 135. London, UK, 2008.
4. Hooper CE, Lyburn ID, Searle J, Darby M, Hall T, Hall D et al. The
South West Area Mesothelioma and Pemetrexed (SWAMP) trial – A
multi-centre prospective observational study evaluating novel markers
of chemotherapy response and prognostication. *British Journal of
Cancer*, 2015, 112: 1175–1182.
5. Nowak AK. CT, RECIST, and malignant pleural mesothelioma. *Lung
Cancer*, 2005; 49 S1: S37–S40.
6. Giesel FL, Bischoff H, von Tengg-Kobligk H, Weber M-A, Zechmann
CM, Kauczor H-U, et al. Dynamic Contrast-Enhanced MRI of Malignant
Pleural Mesothelioma. *Chest*. 2006; 129;1570-1576.
7. Giesel FL, Choyke PL, Mehndiratta A, Zechmann CM, von Tengg-

- Kobligk, Kayser K et al. Pharmacokinetic analysis of Malignant Pleural Mesothelioma- Initial results of tumor microcirculation and its correlation to microvessel density (CD-34). Acad Radiol. 2008; 15:563-570.
8. Clive AO, Hooper CE, Edey AJ, Morley AJ, Zahan-Evans N, Hall D et al. Randomised Controlled Trial of Intravenous Zoledronic Acid in Malignant Pleural Disease: A Proof of Principle Pilot Study. PLOS ONE | DOI:10.1371/journal.pone.0118569.
 9. Veit-Haibach P, Schaefer NG, Steinert HC, Soyka JD, Seifert B, Stahel RA. Combined FDG-PET/CT in response evaluation of malignant pleural mesothelioma. Lung Cancer 2010; 67:311-317.
 10. R Core Team, R Foundation for Statistical Computing, Vienna, Austria. R: A language and environment for statistical computing. 2014. <http://www.R-project.org>.
 11. Therneau TM, Lumley T. Survival. Survival analysis, including penalised likelihood. R package. <http://cran.r-project.org/web/packages/survival/survival.pdf>
 12. Francis RJ, Byrne MJ, Van Der Schaaf AA, Boucke JA, Nowak AK, Phillips M et al Early prediction of response to chemotherapy and survival in malignant pleural mesothelioma using a novel semi-automated 3- dimensional volume - based analysis of serial 18F - FDG PET scans. Journal of Nuclear Medicine. 2007. 48(9): 1449-1458.
 13. Nowak AK, Francis RJ, Phillips MJ, Millward MJ, van der Schaaf AA,

- Boucek J et al. A novel prognostic model for Malignant Mesothelioma incorporating quantitative FDG-PET Imaging with Clinical Parameters. Clin Cancer Research 2010; 16:2409-2417.
14. Lee HY, Hyun SH, Lee KS, Kim B-T, Kim J, Shim YM et al. Volume-based parameter of 18F-FDG PET/CT in Malignant Pleural Mesothelioma: Prediction of therapeutic response and prognostic implications. Ann Surg Oncol 2010; 17:2787-2794.
 15. Gerbaudo VH, Mamede M, Trotman-Dickenson B, Hatabu H, Sugarbaker DJ. FDG PET/CT patterns of treatment failure of malignant pleural Mesothelioma: relationship to histological type, treatment algorithm, and survival. Eur J Nucl Med Mol Imaging. 2011; 38:810-821.
 16. Terada T, Tabata C, Tabata R, Okuwa H, Kanemura S, Shibata E et al. Clinical Utility of 18-fluorodeoxyglucose positron emission tomography/computed tomography in malignant pleural mesothelioma. Experimental and Therapeutic Medicine 2012; 4:197-200.
 17. Abe Y, Tamura K, Sakata I, Ishida J, Ozeki Y, Tamura A et al. Clinical implications of 18F-fluorodeoxyglucose positron emission tomography/computed tomography at delayed phase for diagnosis and prognosis of malignant pleural mesothelioma. Oncology Reports. 2012; 27:333-338.
 18. Abakay A, Komek H, Abakay O, Palanci Y, Ekiki F, Tekbas G et al. Relationship between 18 FDG PET-CT findings and the survival of 177

patients with malignant pleural mesothelioma. *Eur Rev Med Pharmacol Sci.* 2013; 17:1233-1241.

19. Klabatsa A, Chicklore S, Barrington SF, Goh V, Lang-Lazdunski L, Cook GJR. The association of 18F-FDG PET/CT parameters with survival in malignant pleural mesothelioma. *Eur J Nucl Med Mol Imaging.* 2014; 41:276-282.
20. Lopci E, Zucali PA, Ceresoli GL, Perrino M, Giordano L, Gianoncelli L et al. Quantitative analyses at baseline and interim PET evaluation for response assessment and outcome definition in patients with malignant pleural mesothelioma. *Eur J Nucl Med Mol Imaging* (2015) 42:667–675.
21. Kwek B.H. Aquino S.L. Fiscman A.J. Fluorodeoxyglucose Positron Emission Tomography and CT after talc pleurodesis. *Chest.* 2004; 125: 2356-2360.
22. Francis R, Nowak A, Segard T, Morandea L, Lee G, Boucek J et al. Characterization of the effect of pleurodesis on FLT and FDG PET/CT imaging in malignant pleural mesothelioma (MPM). *J Nucl Med* 2014; 55 Suppl 1: 457.
23. Brown J, Buckley D, Coulthard A, Dixon AK, Dixon JM, Easton DF et al. Magnetic resonance imaging screening in women at genetic risk of breast cancer: imaging and analysis protocol for the UK multicentre study. *Magnetic Resonance Imaging.* 2000; 18:765-776
24. Baum F, Fischer U, Vosschenrich R, Grabbe E. Classification of

hypervascularized lesions in CE MR imaging of the breast. *Eur Radiol.* 2002; 12:1087-1092.

25. Walker-Samuel S, Leach MO, Collins DJ. Evaluation of response to treatment using DCE-MRI: the relationship between initial area under the gadolinium curve (IAUGC) and quantitative pharmacokinetic analysis. *Phys Med Biol.* 2006; 51: 3593-3602.

Figure Captions:

Figure 1A MRI axial image showing region drawn over whole of tumour.

Figure 1B Intensity vs frame curve from DCE-MRI study.

Figure 2 FDG PET/CT showing axial, sagittal and coronal planes through the tumor, and MTV definition at above SUV threshold of 2.5

Figure 3 Comparison of Integrated Area Under the first 90 seconds of the DCE-MRI enhancement-time curve (iAUC90) with the SUVmax.

Figure 4 Comparison of Washout rate (%/minute) of the DCE-MRI enhancement-time curve with the SUVmax.

Figure 5 Kaplan Meier analysis, chemotherapy patients, for SUVmax with Overall Survival.

Figure 6 Kaplan Meier analysis, chemotherapy patients, for iAUC90 with Overall Survival.

Figure 7 Kaplan Meier analysis, chemotherapy patients, for washout curve shape with Overall Survival.

Figure 8 Kaplan Meier analysis, chemotherapy patients, for SUVmax and washout curve shape with Overall Survival.

Table Captions:

Table 1. Patient characteristics. Key: CT – computed tomography; IMIG – International Mesothelioma Interest Group; TNM – Tumour Node Metastasis stage; WHO World Health Organisation.

Table 2. Cox regression analysis. * indicates statistical significance. Multivariate analysis was carried out without Histology.

Table 3. Kaplan-Meier analysis of a combination of SUVmax from PET/CT and washout slope from DCE-MRI for treated patients, based on survival time from trial entry to death.

Table 4: Change of PET/CT and DCE-MRI parameters post-treatment compared for patients with disease progression and progression-free at 7-9 weeks post-trial commencement.

Table 5. Change of PET/CT and DCE-MRI parameters post-treatment compared for patients with disease progression and progression-free at 15 weeks post-trial commencement.

Table 6. Change of PET/CT and DCE-MRI parameters post-treatment compared for patients with disease progression and progression-free at 9 months post-trial commencement.

	Chemotherapy arm	Comparator arm
Number of patients	58 (6 female)	15 (4 female)
Age (median(IQR))	69 (65-73)	77 (68-80)
Talc pleurodesis before trial entry	21 (36%)	6 (40%)
Histology		
Epithelioid	39 (67%)	11 (73%)
Sarcomatoid	15 (26%)	0 (0%)
Biphasic	4 (7%)	4 (26%)
Baseline WHO PS		
0	17 (29%)	2 (13%)
1	37 (64%)	11 (73%)
2	4 (7%)	2 (13%)
CT IMIG TNM stage		
I	7 (12%)	1 (7%)
II	4 (7%)	1 (7%)
III	28 (48%)	6 (40%)
IV	19 (33%)	7 (47%)

Table 1. Patient characteristics. CT – computed tomography; IMIG – International Mesothelioma Interest Group; TNM – Tumour Node Metastasis stage; WHO World Health Organisation.

	Univariate		Multivariate	
OS analysis	p-value	HR (95% CI)	p-value	HR (95% CI)
Histology - Sarcomatoid	<0.0001*	3.9 (2.0-7.8)		
Histology - Biphasic	0.0003*	8.5 (2.6-27.2)		
Pleurodesis	0.73	0.90 (0.49-1.64)		
SUVmax	0.005*	1.10 (1.03-1.17)	0.046	1.08 (1.00 – 1.16)
MTV	0.0009*	1 (1-1.001)	0.12	1.0013 (0.9997-1.003)
TLG	0.002*	1 (1.00 – 1.00)	0.25	1.00 (1.00-1.00)
IAUC90	0.22	1.008 (0.995-1.02)		
Washout slope	0.144	0.89 (0.77-1.04)		

Table 2. Cox regression analysis. * significant. Multivariate analysis carried out without Histology.

SUVmax	Washout Slope Type	N	Events	Median OS	95% LCL	95% UCL
<10.6	1	8	4	735	562	NA
<10.6	2	2	2	426	355	NA
<10.6	3	15	11	401	232	NA
>10.6	1	4	4	312	192	NA
>10.6	2	4	4	130	93	NA
>10.6	3	15	14	268	250	493

Table 3.

PFS 7-9 weeks (after three	Progression	Progression free and alive	p-value
----------------------------	-------------	----------------------------	---------

cycles)	mean change	mean change	
SUVmax	-1.3	-2.4	0.40
MTV (ml)	-292	-430	0.45
TLG (SUV-ml)	-1502	-2065	0.54
iAUC90 (%-min)	-0.7	-10.8	0.32
Washout Slope (%/min)	-0.4	1.2	0.03

Table 4.

PFS 15 weeks (after chemo)	Progression mean change	Progression free and alive Mean change	P-value
SUVmax	-1.7	-2.1	0.81
MTV (ml)	-386	-383	0.99
TLG (SUV-ml)	-1871	-1900	0.98
iAUC90 (%-min)	-0.6	-15.5	0.14
Washout Slope (%/min)	0.01	1.3	0.13

Table 5.

PFS 9 months	Progression mean change	Progression free and alive Mean change	p-value
SUVmax	-2.4	-0.4	0.22
MTV (ml)	-463	-151	0.02
TLG (SUV-ml)	-2304	-628	0.01
iAUC90 (%-min)	-5.8	-14.9	0.37
Washout Slope (%/min)	0.28	1.78	0.31

Table 6.

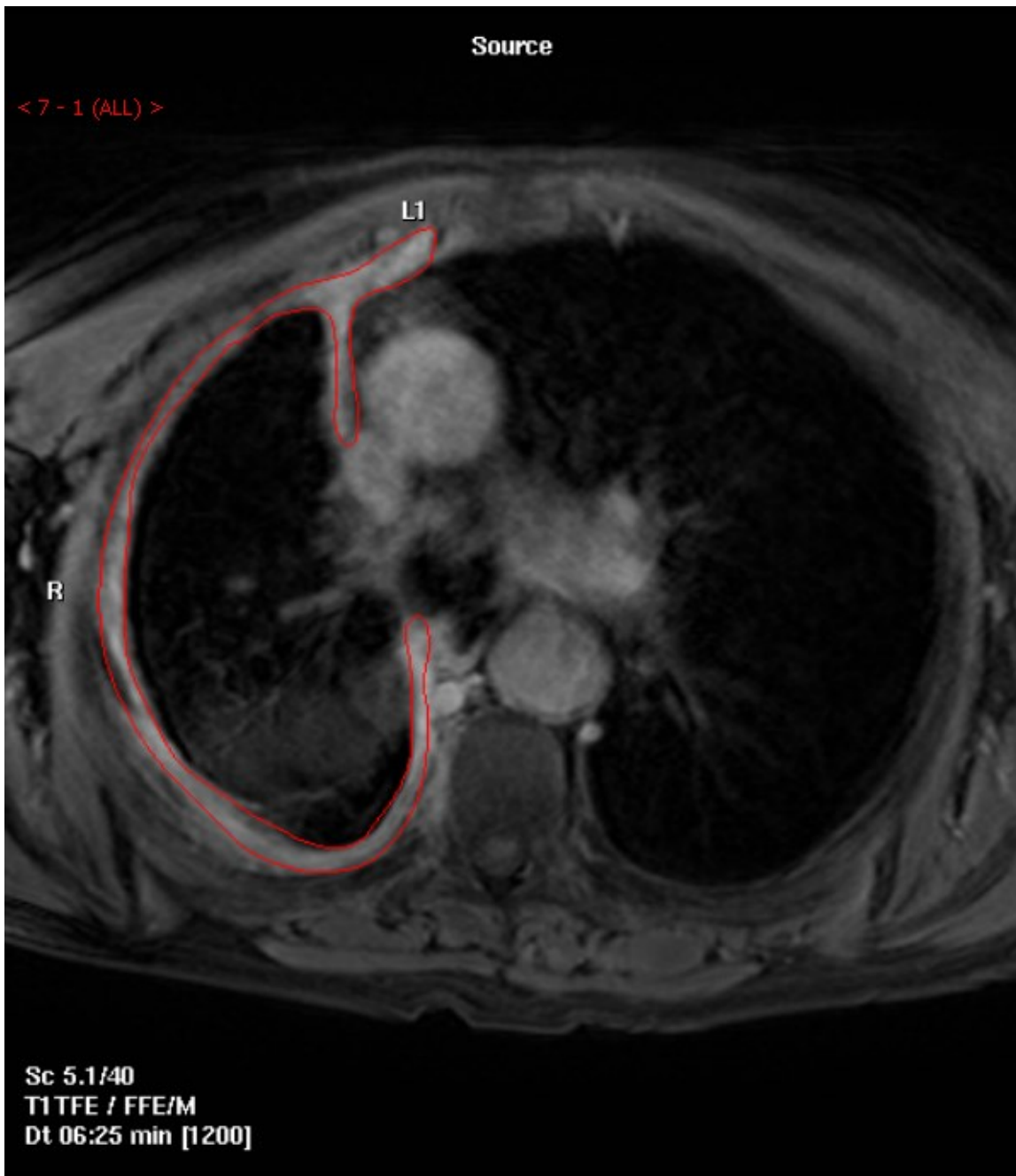


Fig 1A

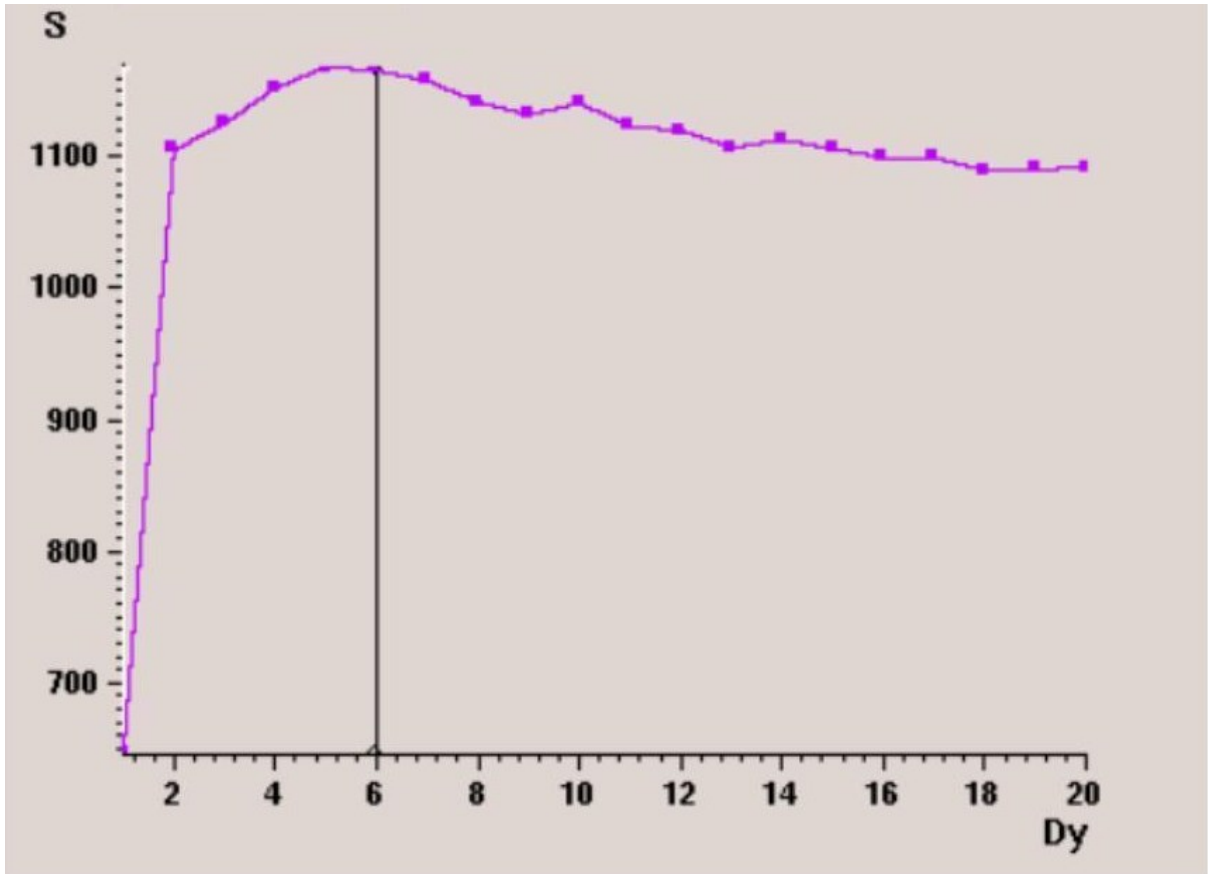


Fig 1B

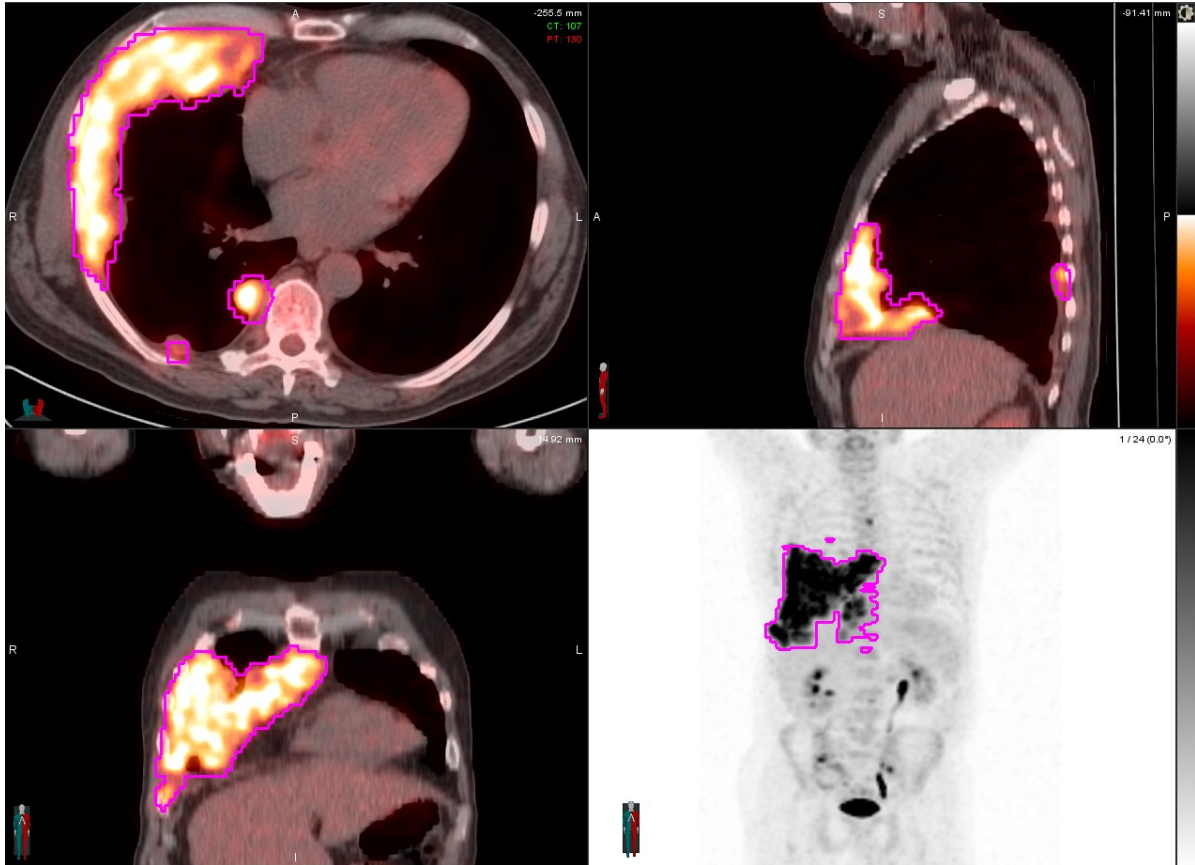


Fig 2

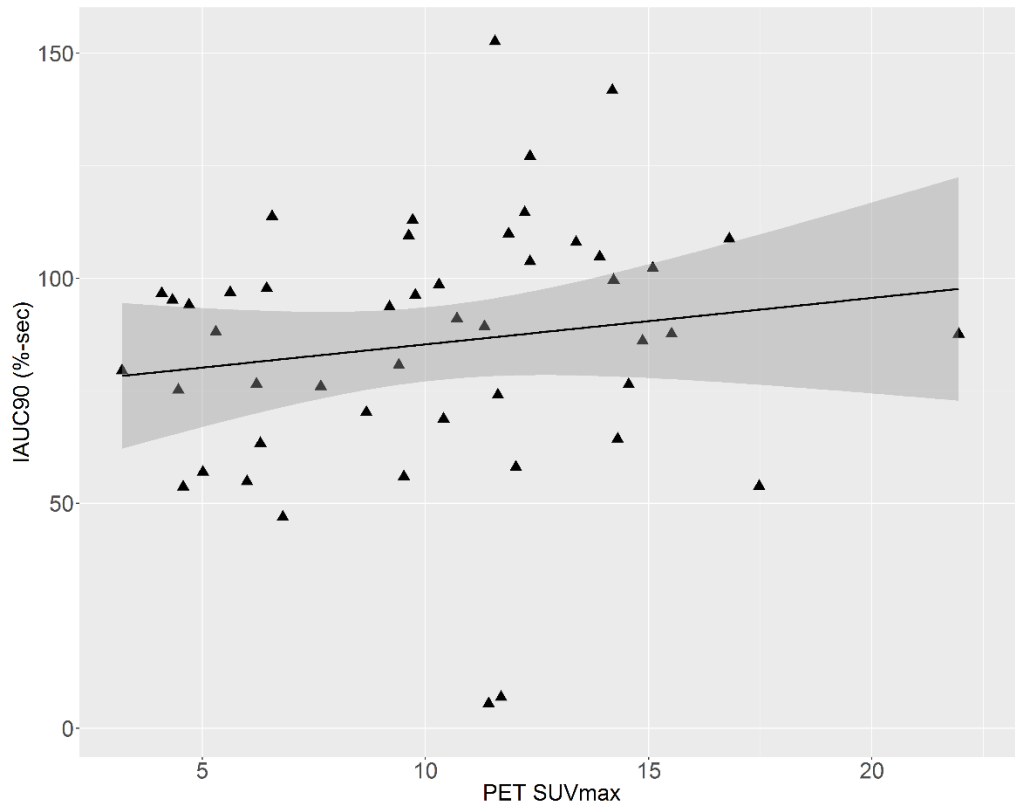


Fig 3

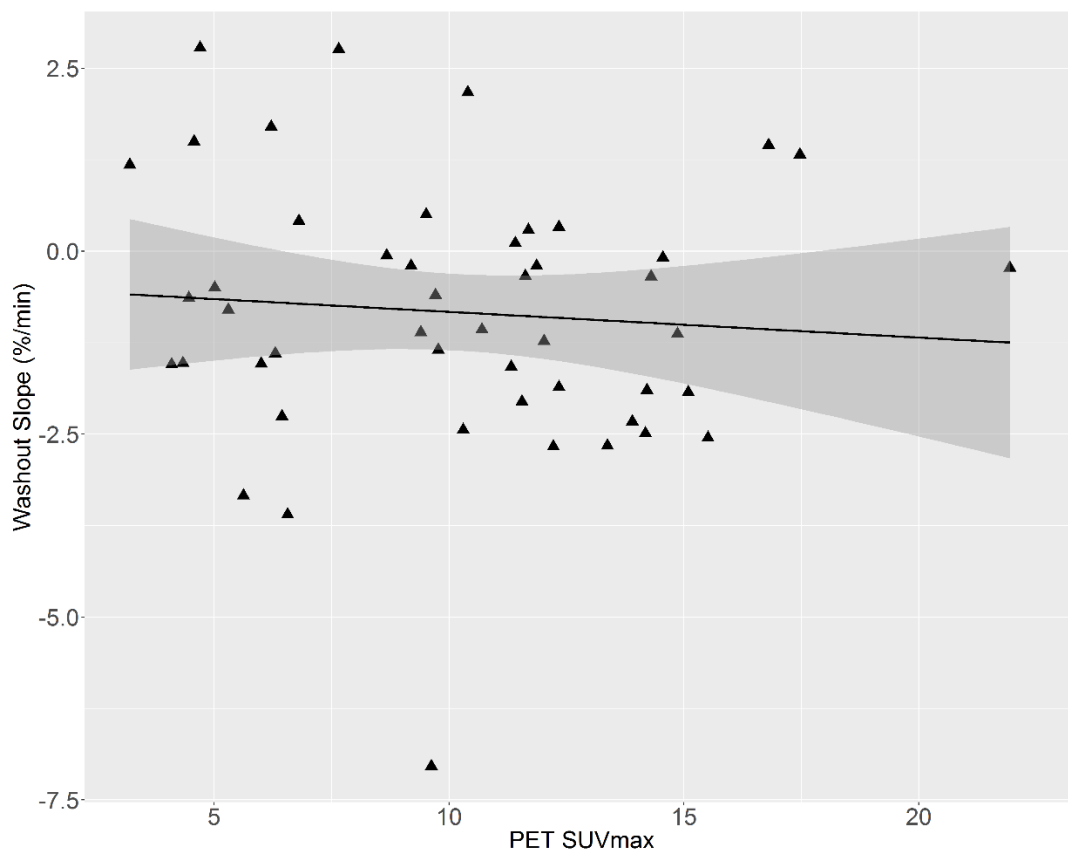


Fig 4

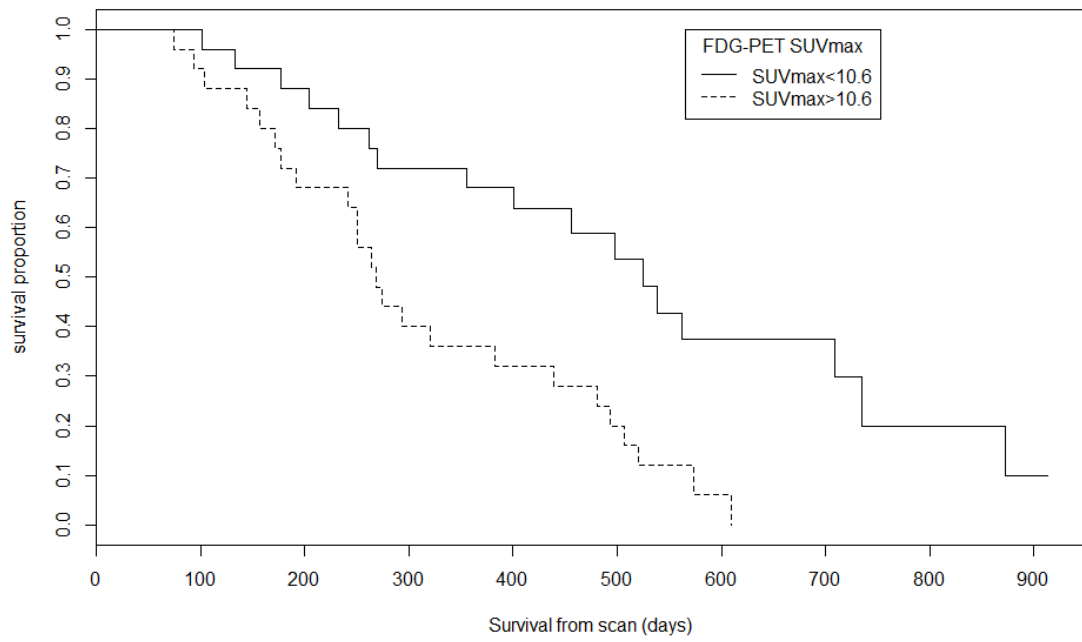


Fig 5

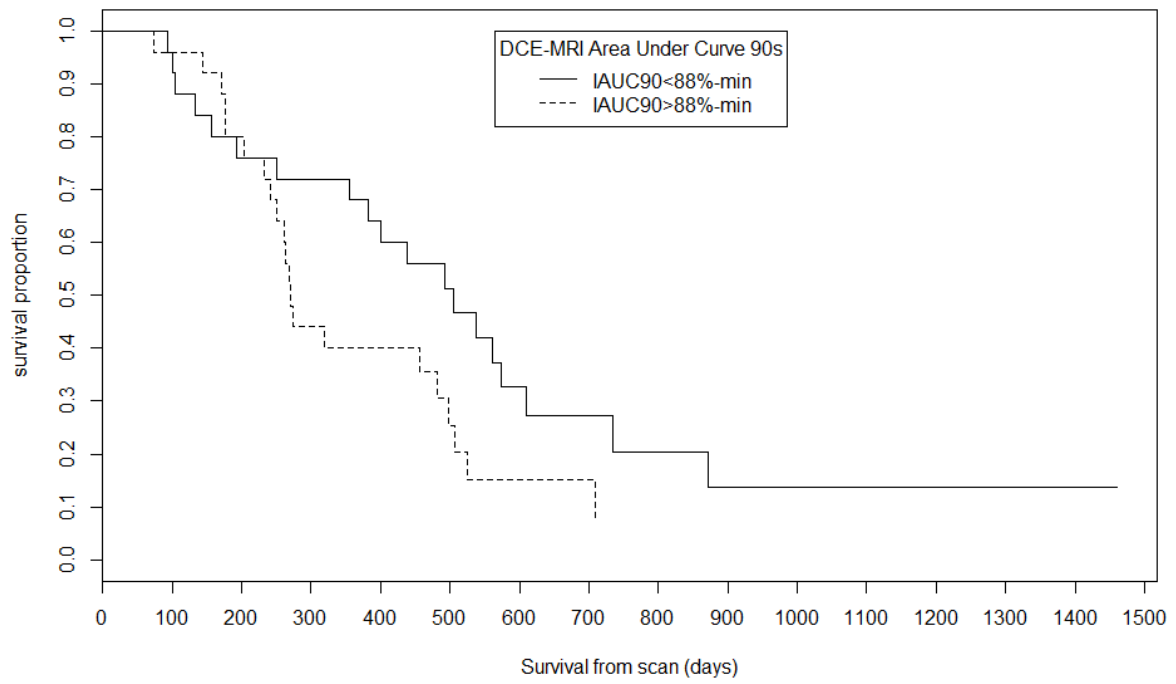


Fig 6

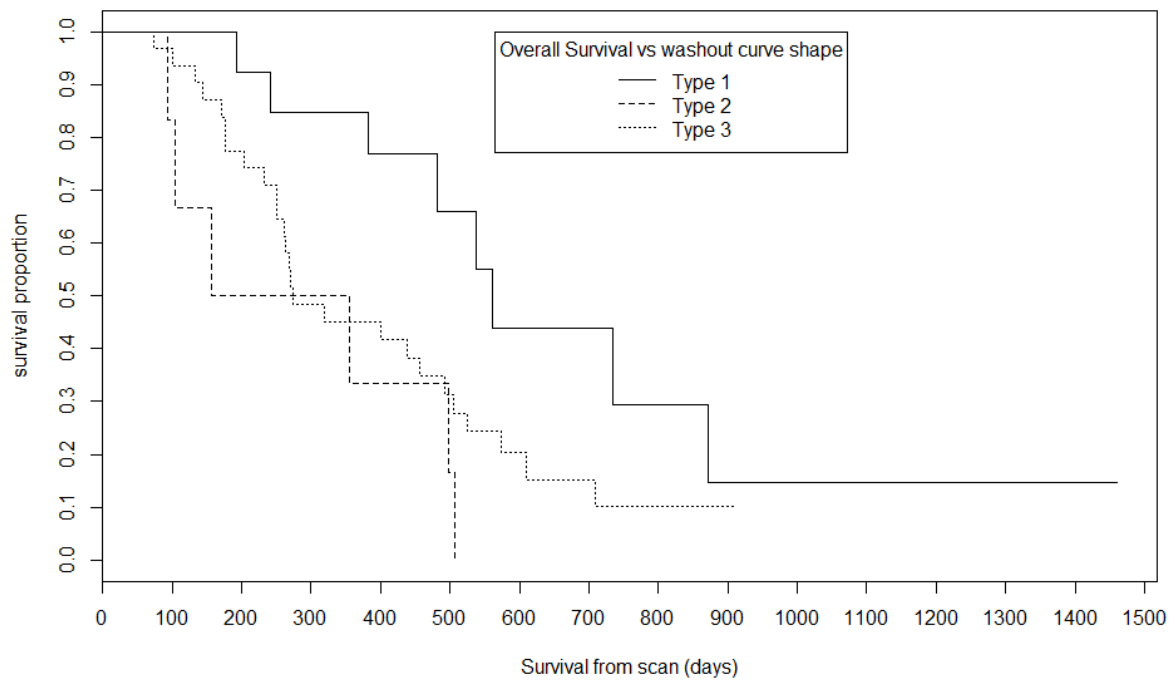


Fig 7

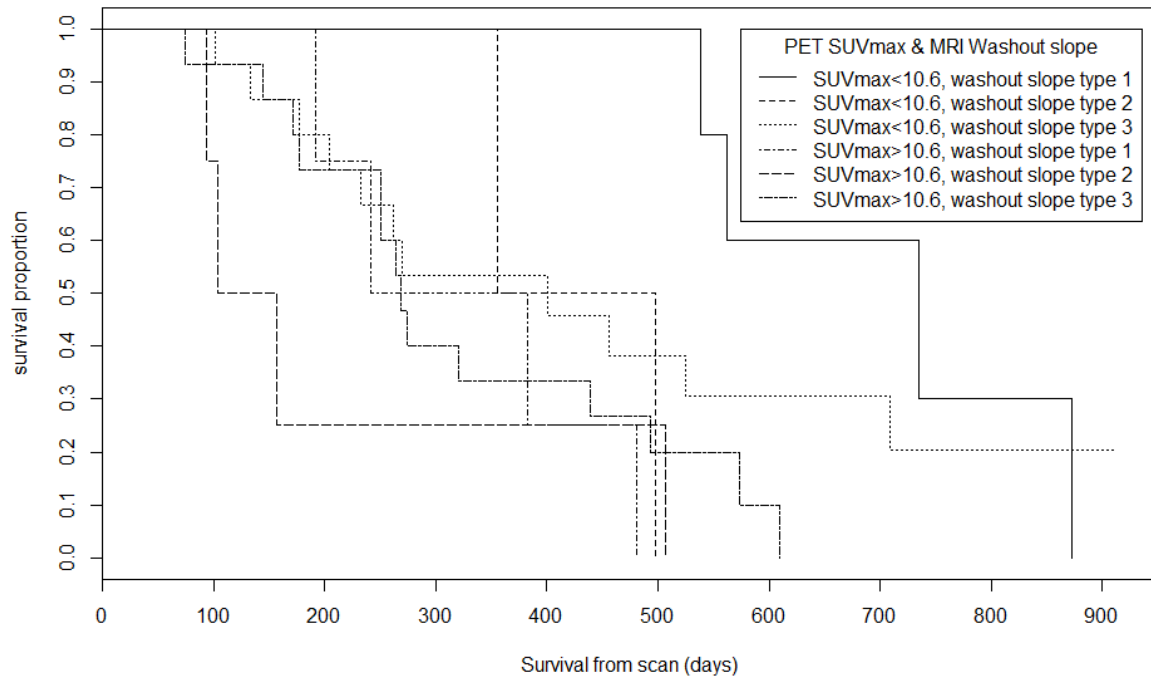


Fig 8